Stress Transfer between FRP Laminates and Concrete through Deteriorated Concrete Surfaces

Amnon Katz[1]

Abstract: This study investigated the mechanism of stress transfer between glass and carbon fiber-reinforced polymer (FRP) laminates and concrete beams with deteriorated surfaces. Thirty-six beams were prepared with either a solid concrete cross section, or with a weak concrete layer at the surface, simulating the state of a deteriorated surface. The beams were reinforced with glass or carbon FRP sheets and tested in flexure. Strain development in the laminate and in the concrete layers was recorded and analyzed. The mode of failure changed from shear within the deteriorated layer of concrete to delamination at the interface between the resin and the concrete in the solid high-strength concrete. A significant amount of stress was transferred between the FRP laminates and the concrete surface probably by residual frictional stresses after shear cracks developed in the deteriorated layer, leading to a remarkable load bearing capacity of these beams.

DOI: 10.1061/(ASCE)1090-0268(2007)11:4(410)

CE Database subject headings: Stress; Fiber reinforced polymers; Laminates; Deterioration; Bearing capacity.

Introduction

Fiber-reinforced polymers (FRPs) are widely used today to strengthen reinforced concrete in situations where the internal reinforcement has corroded or to upgrade existing structures so that they may carry additional loads. In many cases, the concrete at the surface of the existing reinforced concrete (RC) elements suffers from deterioration that, by itself, does not pose any risk to the structure, but forms a separating layer between the "healthy" concrete at the core of the structure and the reinforcing system applied externally to the structure.

Many studies have been conducted to investigate the mechanism of stress transfer between concrete and the external reinforcement, initially with steel sheets (Swamy et al. 1987; VanGemert and Vanden 1986; Eberline et al. 1988) and more recently with FRP (Horiguchi and Saeki 1997; Chen et al. 2001; Xie and Karbhari 1998; De Lorenzis et al. 2001). These researchers realized the importance of proper stress transfer between the reinforcing system and the concrete.

Two major mechanisms of bond failure were identified for strengthened RC beams: Shear failure of the laminate–concrete interface and failure due to ripping of the concrete at the end of the reinforcement, adjacent to the beam supports (Smith and Teng 2002). The results of these studies led to the development of the *ACI Guide for the Design and Construction of Externally Bonded FRP Systems* (ACI 2002), which recommends a minimum of 17 MPa for concrete compressive strength at the surface of the element to be strengthened. Models predicting the behavior of externally reinforced beams were developed, most of which deal with the overall behavior of a beam made of concrete (either cracked or solid) that is considered to be uniform throughout its cross section (Rabinovitch and Frostig 2000; Mukhopadhyaya and Swamy 2001; Etman and Beeby 2000). Other studies, which specifically investigated the bond and stress transfer between external bonded sheets and concrete bodies, also dealt with solid bodies of concrete (Horiguchi and Saeki 1997; Chen et al. 2001; Xie and Karbhari 1998; De Lorenzis et al. 2001; Jia et al. 2005). According to the model developed by Bizindavyi and Neale (1999), the shear force between the FRP laminate and the concrete is transferred across a zone about 2–3 mm thick, thereby forming a separating zone whose mechanical properties must be taken into account when calculating the mechanism of stress transfer. Some researchers attributed the mechanical properties of this layer solely to the resin used to bond the FRP sheet to the concrete, although the properties of the concrete at the surface are generally different from those of the bulk concrete (De Lorenzis et al. 2001).

The complexity of the stress state between FRP reinforcement and concrete led to a variety of test setups, ranging from direct shear pulling to flexural beam tests, as reviewed by Horiguchi and Saeki (1997) and Chen et al. (2001). In the direct shear test, a piece of FRP coupon is bonded to a block of concrete and direct shear load is applied along the sheet in various configurations. In this arrangement, the concrete block is generally subjected to compression, which is unlikely to occur in concrete members subjected to flexure. In the flexural beam tests, the FRP sheet is bonded to the bottom of a concrete beam and the test is carried out by subjecting the beam to flexure, also in various configurations. The flexural tests simulate more accurately the stress development in real applications, although the interpretation of results is more difficult due to the additional forces and moments that are involved in flexure.

The current study tested the stress transfer between carbon and glass FRP laminates and the surface of deteriorated concrete beams. FRP laminates are widely used to strengthen concrete

[1]National Building Research Institute, Faculty of Civil and Environmental Engineering, Technion–Israel Institute of Technology, Haifa 32000, Israel. E-mail: akatz@technion.ac.il

Note. Discussion open until January 1, 2008. Separate discussions must be submitted for individual papers. To extend the closing date by one month, a written request must be filed with the ASCE Managing Editor. The manuscript for this paper was submitted for review and possible publication on December 12, 2005; approved on July 13, 2006. This paper is part of the ***Journal of Composites for Construction***, Vol. 11, No. 4, August 1, 2007. ©ASCE, ISSN 1090-0268/2007/4-410–418/$25.00.

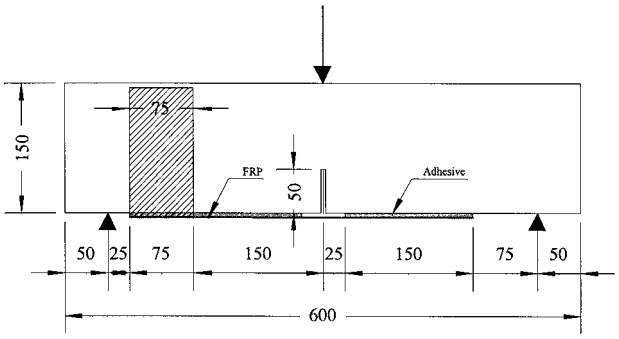

Fig. 1. Experimental setup

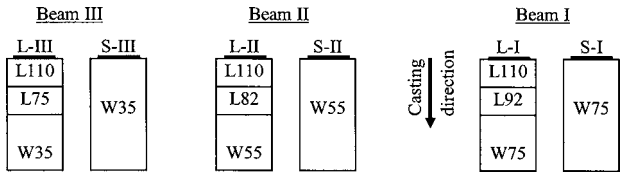

Fig. 2. Cross section of test beams according to concrete types (not to scale). The numbers present the various water/cement ratios.

structures in various cases of severe deterioration of the surface of the concrete elements where the core concrete of such elements remains undamaged. Stress transfer from the surface to the core concrete through layers of varied strength influences the structural behavior of the element. Better understanding of the stress transfer in these cases will enable better design for strengthening of concrete elements.

Experimental Method

Research Program

Thirty-six concrete beams were prepared and strengthened with either glass or carbon FRP laminates. Two types of beams were prepared: Solid and layered. The concrete of the solid beams was uniform throughout the beam, whereas the layered beams were prepared similarly but with a weak concrete layer at the surface. This surface layer was to be strengthened, and it represented a deteriorated surface layer that required repair. The deflection of the beams was tested, as well as stress development in the various layers of concrete and at different locations along the beam. Three different concrete types were used for the bulk concrete and one type was used for the surface layer (see details in the following).

Experimental Setup

Specimens were prepared for three-point flexural tests, as shown in Fig. 1. The specimens consisted of $80\times150\times600$ mm beams made of concrete of three strength levels: 29.7, 46.4, and 76.8 MPa (characteristic compressive strength at 28 days), denoted as I, II, and III, respectively. Two types of beams were prepared: Solid and layered. The solid beams (denoted S) were made with the same concrete throughout the beam's cross section, whereas the layered beams (denoted L) were made similarly but the surface layer, 10 mm thick, was made of a weaker concrete (13.8 MPa). Another layer of concrete was cast between the bulk concrete and the external layer of each of the three beam types, with an intermediate strength level, i.e., 21.5, 27.0, and 29.4 MPa, respectively (Fig. 2). The setup of the layered beams was determined after successful execution of the test program on the solid beams to ensure failure in the bonded area only. The theoretical flexural strength of the beams was 52 and 45 kN for CFRP and GFRP reinforced beams, assuming perfect bond; and the theoretical shear strength calculated according to ACI 318 (including a safety factor) is 22, 27, and 36 kN for concrete Types I, II, and III. Concrete strength was tested again prior to testing the beams (results are shown in Table 2).

Three identical beams were prepared for each type of concrete as follows:

1. Beams were cast with dimensions of $100\times150\times600$ mm for the solid specimens, and $100\times130\times600$ mm for the layered specimens. Two additional 10-mm-thick layers were cast on the latter, immediately after casting the bulk concrete, ensuring concrete continuity throughout the layers (Fig. 2).
2. Beams were cured for 28 days in a moist environment followed by 6 months in air.
3. A 10 mm layer was sawed off from the sides of the beams to expose their side surface, and a 50 mm notch was sawed at the center of each beam.
4. The concrete surface was cleaned using a steel brush. Low-strength concrete surface was strengthened with a thin layer of epoxy resin.
5. Strips of the tested FRP laminates (60×400 mm) were applied to the concrete surface. The strips were applied unevenly in relation to the notch (225 or 175 mm on either side) to ensure failure on one side only. A bond-breaker zone of 25 mm was kept on both sides of the notch to prevent the formation of local stress concentration near the notch, leaving a testing length of 150 mm (Fig. 1). An additional strip of laminate was applied near the end of the untested side to ensure failure at the other side (the tested one). It should be noted that after testing the first specimen (out of three) of each concrete type, it was decided to apply another strip of strengthening laminate closer to the notch to ensure failure at the tested side.
6. Strain gauges were applied to the exposed side surfaces (Stage 3) of the beams and to the FRP laminates according to the experiment plan, as shown in Fig. 3.

All specimens were tested for three-point flexure at age of approximately 7 months (Fig. 1). The midpoint deflection of the upper side of the beam and the strain at all measuring points were recorded until complete failure.

Materials

Concrete

Concrete was prepared using ordinary Portland cement at different water/cement ratios, representing normal-, medium-, and high- strength concrete (water/cement ratios of 0.75, 0.55, and 0.35, respectively). The concrete for the surface layer of the layered concrete was prepared at a constant water/cement ratio of 1.1, representing a deteriorated concrete layer at the surface of the concrete to be repaired. An intermediate layer of concrete was cast between the bulk concrete and the surface layer, allowing a gradual change of concrete quality from the bulk to the surface

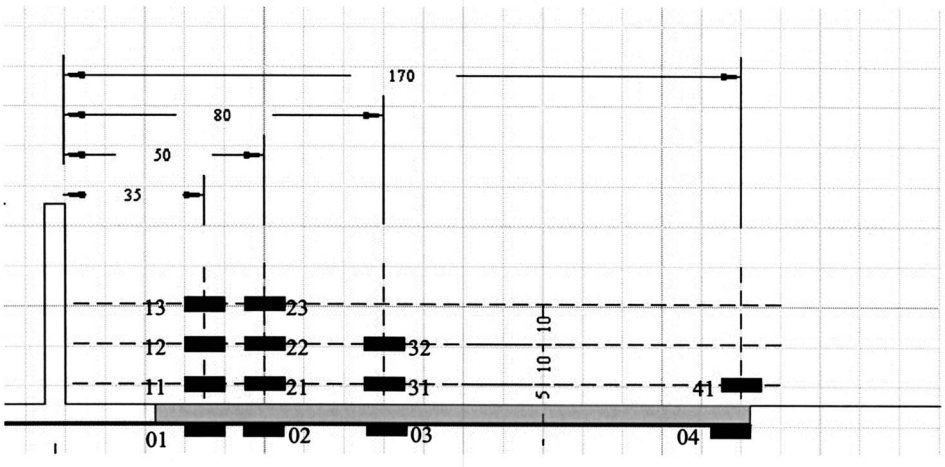

Fig. 3. Setup for strain gauge installation (on both sides of the beam)

(Fig. 2). The thickness of each layer was ~10 mm. All layers were cast continuously to ensure proper bonding between the layers.

The concrete representing the deteriorated surface was designed to achieve marginal mechanical properties with respect to the recommendations in ACI 440.2R. The compressive strength and tensile strength determined by pullout (according to ASTM C-1583, with a 50 mm disk) were slightly lower then the minimal values recommended (14.3 and 1.23 MPa compared with 17 and 1.4 MPa, respectively).

FRP

Carbon and glass fiber reinforced (CFRP/GFRP) laminates were used in this study. Their properties are listed in Table 1. Wet application was done by impregnating the FRP sheets with epoxy resin and then installing them over the concrete surface, following the recommendations in ACI 440.2R-02 (2002) and taking special care to remove entrapped air bubbles.

Table 1. Properties of FRP Systems (Manufacturer's Data)

Property	Carbon fiber fabric	Glass fiber fabric	Epoxy resin	Carbon fiber laminate	Glass fiber laminate
Tensile strength (MPa)	3,800	3,100	72.4	876	575
Modulus of elasticity (GPa)	228	76	3.18	72.4	26.1
Elongation (%)	1.6	4.9	5.0	1.21	2.2
Typical thickness (mm)				1.0	1.3

Results

Modes of Failure

Three modes of failure were identified (Fig. 4) and are summarized in Table 2:

- Mode 1: Failure of the epoxy–concrete interface only;
- Mode 2: Failure of the concrete surface layer; and
- Mode 3: Diagonal shear failure of the beam, starting close to the end of the laminate.

Solid beams: Some concrete crumbs were found to adhere to the end of the laminate in beams that failed through Mode 1. These crumbs indicate local tensile stresses that developed near the end of the laminate (Rabinovitch and Frostig 2000; Nguyen et al. 2001). Failure of the epoxy–concrete interface was typical to the solid beams made of high-strength concrete (S-III) reinforced with carbon or glass FRP. Mode 1 was also identified in the failure of medium-strength solid beams (S-II) reinforced with GFRP. The weaker solid beams (S-I for GFRP and S-I and S-II for CFRP) failed through Mode 2, i.e., failure of the concrete layer just below the surface of the beam.

Layered beams: The layered beams failed either through shearing of the entire beam (Mode 3) or by failure of the concrete surface layer (Mode 2). This layer was characterized by low strength, typical to deteriorated concrete; thus, failure of this layer is to be expected after successfully testing the solid beams and the shear failure in Mode 3 was unexpected. This kind of failure resulted probably from a crack that started to develop in the deteriorated layers near the end of the laminate as was characterized

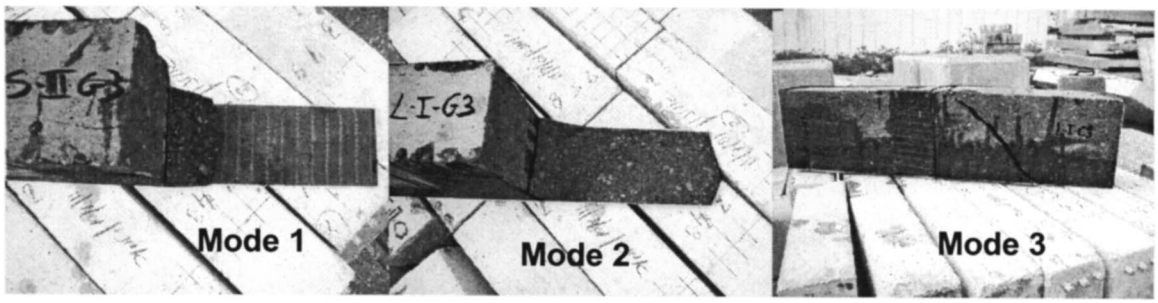

Fig. 4. Three modes of failure

Table 2. Failure Modes and Ultimate Loads Obtained for Test Beams

Type of laminate	Type of beam	Designation	Concrete strength[a] (MPa)	Average ultimate load (kN)	Mode of failure[b]
Carbon	Layer	L-I-C	30.5	27.8	3/3/2
		L-II-C	51.4	26.4	3/3/2
		L-III-C	83.8	20.7	2/2/2
	Solid	S-I-C	30.5	25.3	2/2/2
		S-II-C	51.4	24.1	2/2/2
		S-III-C	83.8	31.4	1/1/1
Glass	Layer	L-I-G	30.5	21.8	3/3/2
		L-II-G	51.4	22.5	2/2
		L-III-G	83.8	22.4	2/2/3
	Solid	S-I-G	30.5	19.0	2/2/2
		S-II-G	51.4	24.0	1/1/1
		S-III-G	83.8	21.2	1/1/1

[a]At the test day of the beams (~7 months).

[b]Results from all test beams. 1=failure of epoxy–concrete interface; 2=failure of concrete at the surface; and 3=shear of the whole beam.

by Smith and Teng (2002). Upon propagation of this crack, the cross section of the beam decreased and the remaining cross section was unable to support the load, which in turn led to further propagation of the crack until failure by shear of the entire beam. Failure through Mode 3 was more pronounced with the normal- and medium-strength concretes. When the bulk beam was strong enough to support the shear load noted previously, a crack developed along the weak layer of concrete until failure occurred through Mode 2.

It should be noted that other types of shear cracks developed near the notch upon loading of the beams, resulting from the development of tensile stress near the free edge of the notch, as can be seen in the photo of Mode 1 in Fig. 4. No additional cracks, such as flexural cracks, were identified along the beam besides the above-mentioned cracks.

Ultimate Load

Table 2 presents the average ultimate loads of all beams tested (Fig. 5). The average for the layered beams was calculated based on the results of the second and third specimens of each concrete type only, due to differences in the failure mode of the layered beams of the first specimen, which required additional strengthening of the anchored side as noted previously. Solid beams: Concrete strength did not affect the bearing capacity of glass fiber reinforced solid beams (Fig. 5). In the case of carbon fiber reinforced solid beams, a higher bearing capacity was observed in beams S-III with the stronger concrete. The mode of failure changed from Mode 2 to Mode 1 with the increase in concrete strength, which could lead to better exploitation of the stiffer laminate.

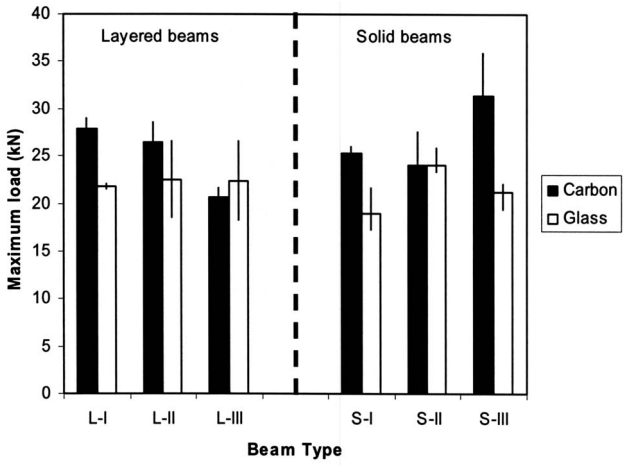

Fig. 5. Ultimate load of strengthened beams

Layered beams: The ultimate load of all glass fiber reinforced beams was similar whether they had a deteriorated or nondeteriorated surface (i.e., layered or solid beam), regardless of the different concrete strengths (Fig. 5). A decrease in the ultimate load was seen, however, for the carbon fiber reinforced layered beams as concrete strength increased. As the surface concrete of all layered beams was the same, a similar ultimate load was expected for all layered beams regardless of the concrete strength of the bulk concrete under the weaker layer. It appears that increasing the difference between the mechanical properties of the concrete surface layer and the CFRP laminate on one side, and between the concrete surface layer and the bulk concrete on the other side, led to a decrease of up to 25% in the bearing capacity of the beam. This decrease was not observed when the beam was reinforced with a GFRP laminate with a lower stiffness than that of the CFRP. According to the model developed by Bizindavyi and Neale (1999), a steep strain gradient may develop in a soft layer that transfers shear stress between two stiff layers (e.g., carbon laminate and high-strength concrete). This gradient becomes more moderate when one of the stiff layers becomes softer, as in the case of weaker concrete or low modulus fibers. This reduction in the strain gradient may explain the increase in bearing capacity of CFRP beams as concrete strength decreased.

This observation is of special interest as the mode of failure of these beams also changed from Mode 3 to Mode 2, i.e., from shear failure at a relatively high ultimate load for beams with weak bulk concrete to failure at the surface layer but at lower ultimate loads for beams with strong bulk concrete. It appears that when the bulk concrete was stronger and stiffer, smaller loads could be transferred through the weak concrete surface.

Load Deflection

Figs. 6(a and b) present the load–deflection behavior of carbon and glass fiber reinforced beams, respectively. Typical to all beams is a plateau at 6–9 kN, probably resulting from the formation of a crack at the notch of the concrete beam. At the onset of this crack, the tensile load carried by the concrete and the laminate was transferred solely to the laminate, leading to increased deflection at that load. The plateau can be associated with the properties of the reinforcing laminate and of the concrete layer at the surface. It was more pronounced in beams reinforced with the low modulus FRP laminates and in the layered beams. Thus, this behavior was most prominent in layered beams reinforced with GFRP and was hardly observed in solid beams reinforced with CFRP laminates.

After crack formation, no significant differences were seen in the load–deflection behavior of the glass fiber reinforced beams, whether solid or layered, besides a slightly greater deflection at the plateau region for the latter, as noted above.

Layered beams reinforced with carbon fibers exhibited greater deflection (lower stiffness) at the post-cracking zone compared with solid beams. The stiffness of the layered beams further decreased as the strength of the bulk concrete decreased, exhibiting

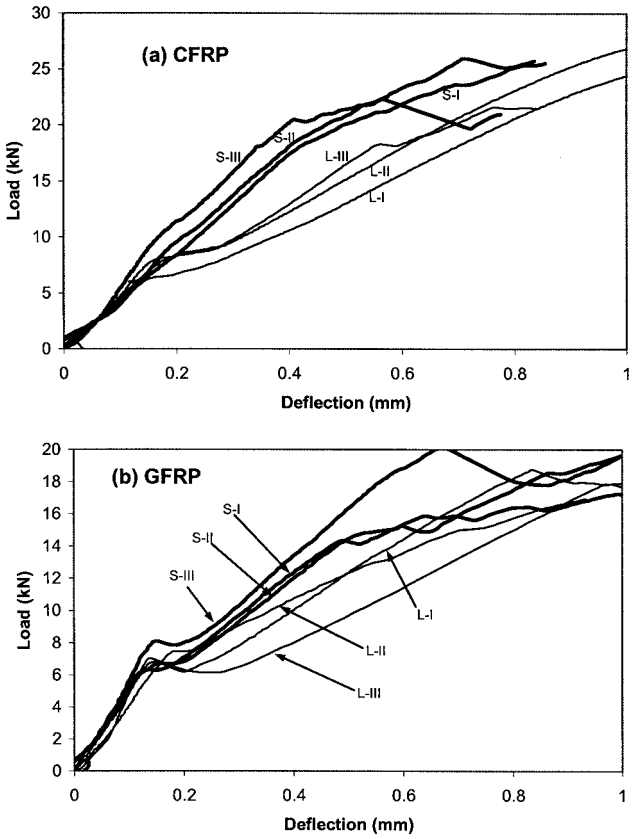

Fig. 6. Load–deflection behavior of (a) carbon; (b) glass fiber reinforced beams

greater deflections at the same load levels. All solid beams exhibited similar behavior, regardless of concrete strength. It appears that concrete properties play an important role in determining the strength and stiffness of deteriorated beams reinforced with high modulus fibers. This effect is less important when the fibers have a lower modulus that is closer to that of concrete.

Strain and Bond Stress Development on Laminate

According to the literature, strain distribution along the laminate drops rapidly from higher strains near the notch to lower strains farther from the notch (Bizindavyi and Neale 1999; Jia et al. 2005; Chen et al. 2001). A similar pattern was seen in this study for the solid beams (Fig. 7). Solid beams reinforced with CFRP exhibited a pattern similar to that of the GFRP, but at different strain levels, due to differences between the modulus of elasticity of the carbon and glass laminates. In order to compare the two laminates, Fig. 7 presents the strain in normalized units relative to the strain measured close to the notch at each loading level (SG #01 in Fig. 3).

In the solid beams, the reduction in strain along the laminate was significant for both kinds of laminate, and the strain measured 55 mm from the notch was only 5–10% compared with that measured at 10 mm, where somewhat more moderate reduction was observed for the CFRP reinforcement. These results were similar at both low and high load levels (Fig. 7). The reduction observed in the layered beams at low load levels was more moderate than that in the solid beams, and it distributed over a larger distance. These findings coincide with the model by Bizindavyi and Neale (1999) for solid and layered beams before bond failure. At high load levels, however, an approximately linear reduction in strain was seen for both laminates. This indicates evenly distributed bond stresses that might be the result of residual frictional stresses. A constant strain level is expected if bond failure

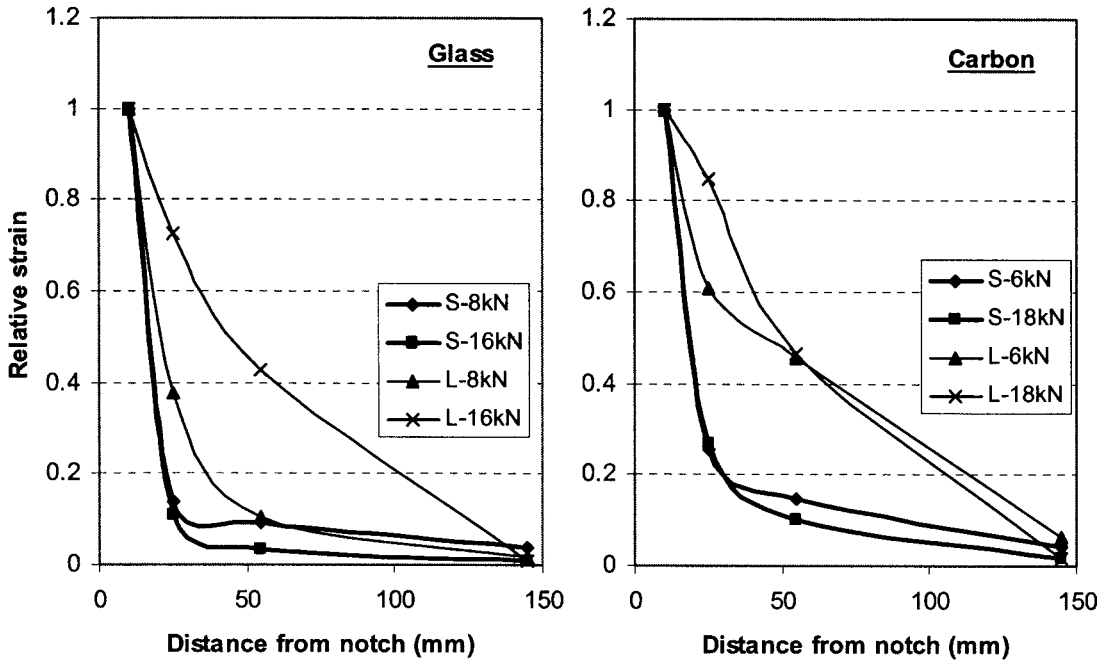

Fig. 7. Comparison between relative strain distribution in the laminate of solid (S) and layered (L) beams reinforced with CFRP and GFRP at various loads

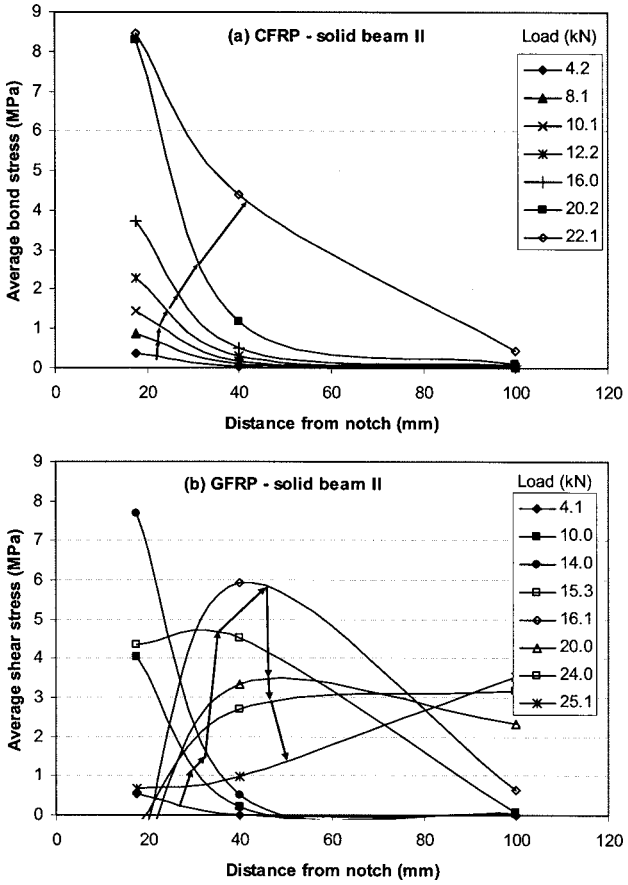

Fig. 8. Development of bond stress in Solid Beam S-II for (a) carbon; (b) glass reinforcement. Arrows show gradual increase of external load.

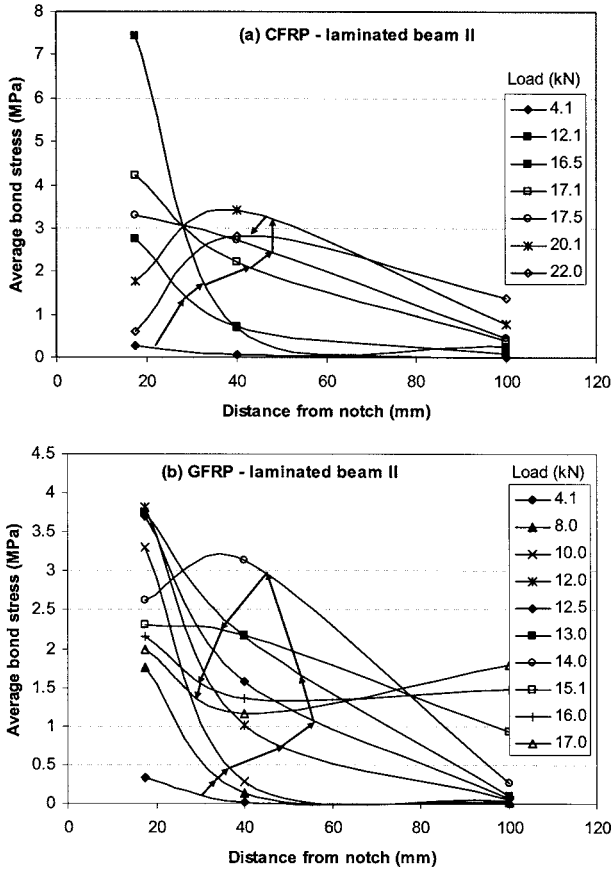

Fig. 9. Development of bond stress in Layered Beam L-II for (a) carbon; (b) glass reinforcement. Arrows show gradual increase of external load.

occurs with no stress transfer along the unbonded area (Jia et al. 2005), whereas linear reduction is more typical to the mechanism of stress transfer by friction.

In order to study the mechanism of stress transfer between the laminate and the concrete, the local average bond stress, τ, was calculated according to the following equation, representing the average bond stress between measuring points 01–02, 02–03, and 03–04 in Fig. 3:

$$\tau = \frac{tE_f(\varepsilon_n - \varepsilon_{n+1})}{l_{n+1} - l_n} \quad (1)$$

where t=laminate thickness (mm); E_f=modulus of elasticity of laminate (MPa); ε_n and ε_{n+1}=measured strain at points n and $n+1$ on the laminate; and l_n and l_{n+1}=distance from the notch to points n and $n+1$ on the laminate.

Figs. 8 and 9 present the development of bond stress along the laminate for carbon and glass FRP laminates in solid (Fig. 8) and layered (Fig. 9) beams. The bond stresses in the CFRP-reinforced solid beam S-II increased gradually with the increase in load [Fig. 8(a)]. The bond stress close to the notch was always at its highest and decreased rapidly with the increase in distance from the notch. Sudden shear failure of the concrete near the notch, between measuring points #01 and #02 and the notch, prevented further monitoring of stress development at higher loads. Prior to that, significantly high bond stress developed suddenly between strain gauges SG #02 and #03 (~40 mm from the notch), indicating the initiation of concrete failure closer to the notch. This was indicated also by stress reduction in the concrete close to the surface (SG #21), as will be discussed later. The failure mode of the beam presented in Fig. 8(a) was Mode 2, i.e., failure of the surface concrete layer.

Bond stress developed similarly also in GFRP-reinforced solid beam S-II but only up to a load of approximately 14 kN [Fig. 8(b)]. Beyond this load, debonding occurred close to the notch, where it was totally reduced, and it continued to increase farther away from the notch. The failure mode of this beam was Mode 1, i.e., failure of the epoxy–concrete interface.

A different development pattern of bond stresses was seen in the layered beams (Fig. 9). Initial increase in the load was accompanied by an increase in bond stress close to the notch. At a certain load, bond stress close to the notch begins to decrease to a certain extent, whereas the stresses farther from the notch continue to increase. The mode of failure of the layered beams shown in Fig. 9 was Mode 2, i.e., failure in the surface concrete layer, which is significantly weaker than the bulk concrete. It appears that although failure of this layer occurred close to the notch, a significant amount of stress could be transferred through that layer, probably by residual frictional stresses. Significantly higher residual stresses are transferred by this mechanism in GFRP versus CFRP. The differences in the modulus of the laminates led to greater strain development in the GFRP laminate and to a greater deflection of the beams (Fig. 6), which in turn led to more stress transfer by friction through the surface layer of concrete. The increase in bond stress seen in the GFRP-reinforced layered beam at the highest loads, after initial reduction, is probably a result

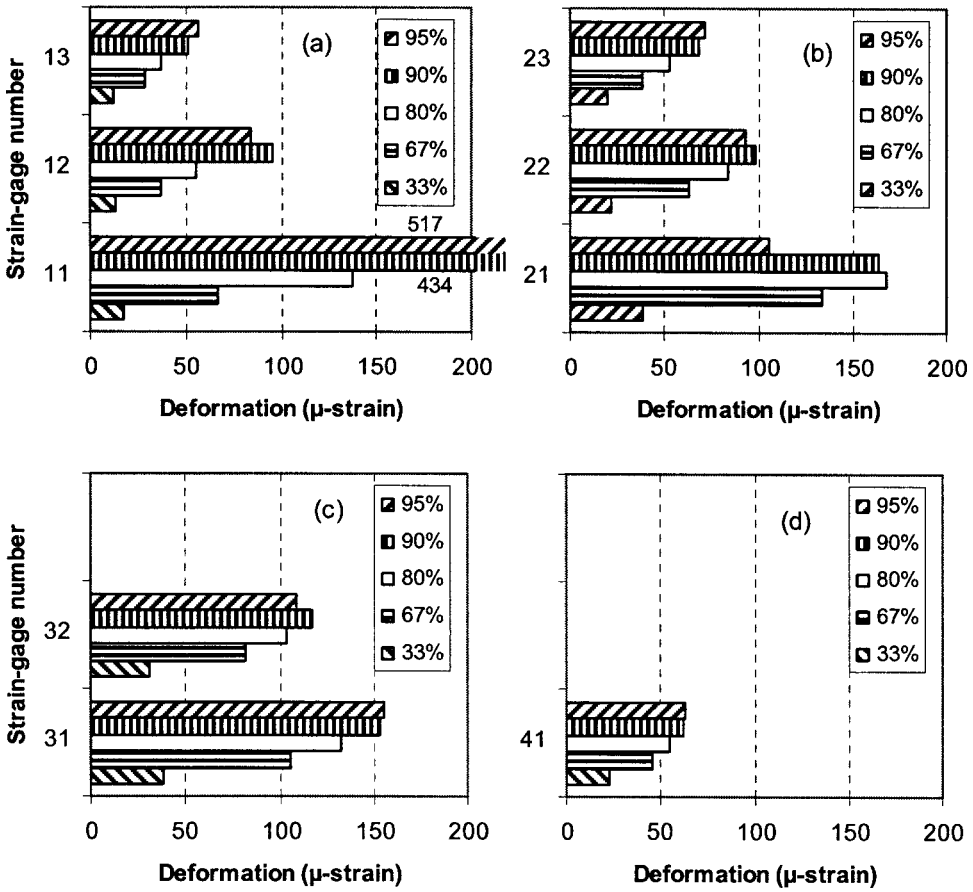

Fig. 10. Development of strain in concrete layers at various locations (for strain gauge number, see Fig. 3). CFRP Solid Beam S-II. Load is expressed as a percentage of the ultimate load (22.3 kN).

of this mechanism [Fig. 9(b)]. Such an increase was not seen in the CFRP beam, as the deflection of this beam is much smaller (Fig. 6).

Stress Distribution in Concrete Layers

Strain development was measured by a series of strain gauges located on both sides of the concrete beam surface, as shown in Fig. 3. Representative results are shown in Fig. 10 and Fig. 11, for solid and layered beams that are reinforced with carbon fiber laminates. Figs. 10 and 11 present the strain development at different load levels and at various locations on the beam's surface.

In the solid beam, the strain at all measuring points increased as the load increased (Fig. 10). It was found that the strains measured by SG #21 at low load levels were greater than those measured by SG #11, indicating an initial stress concentration at some distance from the notch. As the load increased, a significant proportion of the stress was transferred closer to the notch (measured by SG #11) until failure. At high load levels (90 and 95% of the ultimate load), shear cracks started to develop in the concrete near the notch, which led to a significant increase in the strains measured by SG #11 and to some relief of the strains measured farther from the notch (SG #21), until failure of the beam.

Development of horizontal cracks in the external layer of concrete in the layered beams led to a limited capacity of stress transfer (Fig. 11). The concrete layer close to the notch sheared at relatively low loads and a significant proportion of the load was transferred away from the notch (see readings at SG #21 and #31 in Fig. 11). As the load increased to over 67% of the ultimate load, shear occurred in the vicinity of SG #21 and strain readings did not continue to increase in this area. Some stress was still transferred through residual frictional stresses in this area, leading to significant strain readings by SG #21 and #31 whereas zero readings are to be expected if no stress is transferred. This mechanism of shear and friction also led to rapid stress transfer to the hindmost strain gauge SG #41 at relatively low loads (Fig. 11).

Stress development close to the notch (SG #11) was more complicated, as the concrete at the external layer cracked at a relatively low load. The major tensile stress was transferred away from the notch and gradually led to the development of some compression stress closer to the notch. The initial tensile stress near the notch (SG #11 and 12) was therefore suppressed to the extent that some compression stresses developed at SG #11.

Discussion

Studies on the effect of concrete strength on the bond strength between FRP laminates and concrete showed that the average bond strength may increase with the increase in concrete strength (Horiguchi and Saeki 1997, tested for carbon FRP). Similar findings were observed in this study for the case of solid concrete beams reinforced with CFRP. It was found, however, that concrete strength had no effect on the bearing capacity of solid beams reinforced with glass FRP laminates. The mode of failure changed with the increase in concrete strength—from failure within the concrete close to the surface (Mode 2) to failure of the adhesion

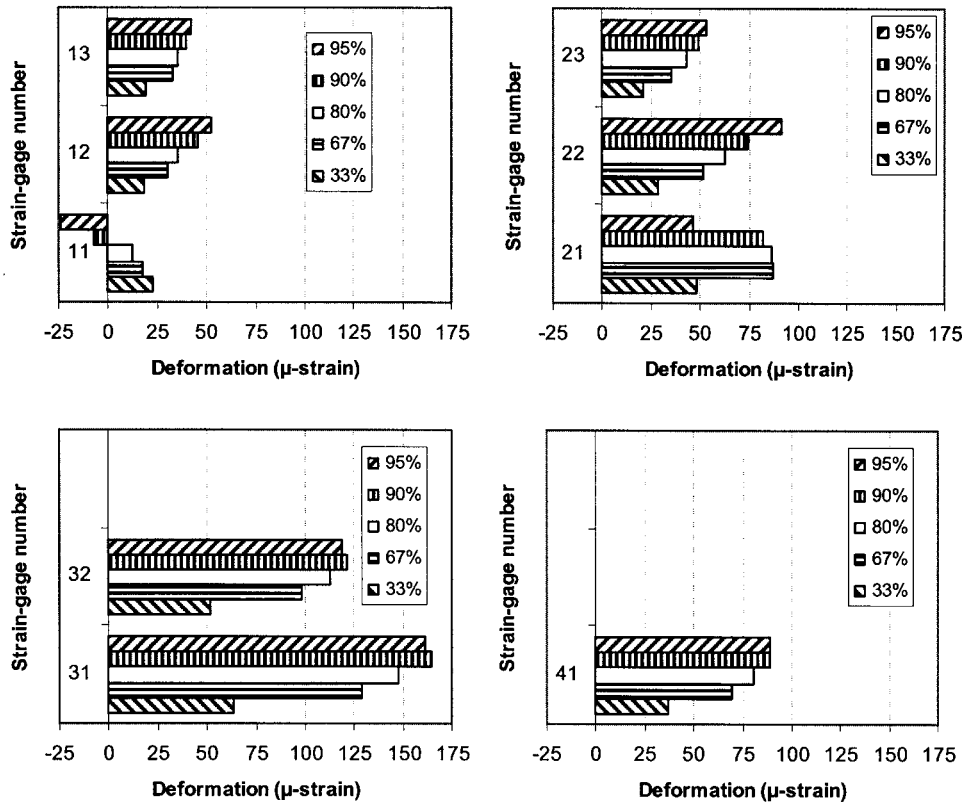

Fig. 11. Development of strain in concrete layers at various locations (for strain gauge number, see Fig. 3). CFRP Layered Beam L-I. Load is expressed as a percentage of the ultimate load (29.0 kN).

between the epoxy and concrete surface (Mode 1), while the bearing capacity remained similar. The development of strain in the high modulus laminate was smaller than that which developed in the lower modulus laminate, leading to better exploitation of the properties of the interfacial zone between the laminate and the bulk concrete.

The layered beams with weak concrete at the surface failed in the weak concrete layer. It seems, however, that a significant amount of stress is transferred by residual frictional stresses through the fractured concrete layer, leading to a bearing capacity of the same order as that of the other solid beams, despite the weaker interface. The mechanism of stress transfer by friction is enhanced by the deflection of the beam that increases the normal stress between the laminate and the concrete. It is therefore possible that beams with less deflection (high-strength concrete beams reinforced with high modulus fibers, e.g., CFRP beam L-III) will exhibit a lower bearing capacity than beams with normal concrete strength, as was found in this study. The deflection of the beam might also be the reason for the larger strain measured farther away from the notch in the external layer of concrete.

Summary and Conclusions

This study experimentally investigated the effect of the deterioration of a concrete surface on the properties of cracked concrete beams externally reinforced by carbon and glass fiber reinforced laminates. The deteriorated layer forms a weak layer that separates the solid and healthy concrete from the reinforcing layer, thus playing an important part in transferring stress between the layers.

It was found that the presence of a weak concrete layer (compressive strength of 14 MPa) that separates between the core concrete (of various strength levels, 30–77 MPa) and the FRP reinforcing system did not significantly affect the bearing capacity of the beams. The effects were in the range of ±25% at the most, but generally, not more than ±15%. It was found that the changes in the bearing capacity could be related to the FRP type. No significant effects of the strength of the bulk concrete away from the surface or of the presence of a weak concrete surface layer were observed with glass FRP reinforcement. The highest bearing capacity of solid beams reinforced with carbon FRP laminate was recorded for the strongest concrete; however, the bearing capacity decreased with the increase of the core strength for beams with a weak concrete surface layer.

The difference between the stiffness of the reinforcing system and that of the concrete surface played an important role in transferring stresses between the layers and in the overall effect on the deflection of the reinforced beam. In the case of a weak concrete layer at the surface, shear stress extended over a greater distance from the crack and the total deflection was larger. A significant proportion of the shear stress was probably transferred by a mechanism of friction (by residual frictional stresses) at the external concrete layer after the formation of shear cracks. Measurements of the longitudinal strain in the layers of concrete indicated a complicated situation of stress transfer with simultaneous action of external and internal shear forces and moments. A model to simulate this stress distribution is currently under development.

References

American Concrete Institute (ACI). (2002). "Guide for the design and construction of externally bonded FRP systems for strengthening concrete structures." *ACI 440.2R-02*, Farmington Hills, Mich.

Bizindavyi, L., and Neale, K. W. (1999). "Transfer lengths and bond strengths for composites bonded to concrete." *J. Compos. Constr.*, 3(4), 153–160.

Chen, J. F., Yang, Z. J., Pan, X. M., and Holt, G. D. (2001). "Effect of test methods on plate-to-concrete bond strength." *Proc., Fibre-Reinforced Plastics for Reinforced Concrete Structures—FRPRCS-5*, C. J. Burgoyne, ed., Vol. 1, Thomas Telford, London, 429–438.

De Lorenzis, L., Miller, B., and Nanni, A. (2001). "Bond of fiber-reinforced polymer laminates to concrete." *ACI Mater. J.*, 98(3), 256–264.

Eberline, D. K., Klaiber, F. W., and Dunker, K. (1988). "Bridge strengthening with epoxy-bonded steel plates." *Transportation Research Record. 1180*, Transportation Research Board, Washington, D.C., 7–11.

Etman, E. E., and Beeby, A. W. (2000). "Experimental program and analytical study of bond stress distributions on a composite plate bonded to a reinforced concrete beam." *Cem. Concr. Compos.*, 22(4), 281–291.

Horiguchi, T., and Saeki, N. (1997). "Effect of test methods and quality of concrete on bond strength of CFRP sheet." *Proc., Non Metallic (FRP) Reinforcement for Concrete Structures*, Vol. 1, Japan Concrete Institute, Tokyo, 265–270.

Jia, J., Boothby, T. E., Bakis, C. E., and Brown, T. L. (2005). "Durability evaluation of glass fiber reinforced-polymer-concrete bonded interfaces." *J. Compos. Constr.*, 9(4), 348–359.

Mukhopadhyaya, P., and Swamy, N. (2001). "Interface shear stress: A new design criterion for plate debonding." *J. Compos. Constr.*, 5(1), 35–43.

Nguyen, D. M., Chan, T. K., and Cheong, H. K. (2001). "Brittle failure and bond development length of CFRP-concrete beams." *J. Compos. Constr.*, 5(1), 12–17.

Rabinovitch, O., and Frostig, Y. (2000). "Closed-form high-order analysis of RC beams strengthened with FRP strips." *J. Compos. Constr.*, 4(2), 65–74.

Smith, S. T., and Teng, J. G. (2002). "FRP-strengthened RC beams. I: Review of debonding strength models." *Eng. Struct.*, 24(4), 385–395.

Swamy, R. N., Jones, R., and Bloxham, J. W. (1987). "Structural behaviour of reinforced concrete beams strengthened by epoxy-bonded steel plates." *Struct. Eng.*, 65A(2), 59–68.

Van-Gemert, D., and Vanden, B. M. (1986). "Long-term performance of epoxy bonded steel-concrete joints." *Proc., Adhesion between Polymers and Concrete*, Chapman and Hall, London, 518–527.

Xie, M., and Karbhari, V. M. (1998). "Peel test for characterization of polymer composite/concrete interface." *J. Compos. Mater.*, 32(21), 1894–1913.